Fish & Shellfish Immunology 47 (2015) 697–705

Contents lists available at ScienceDirect

Fish & Shellfish Immunology

journal homepage: www.elsevier.com/locate/fsi

Full length article

First report on the gastropod proapoptotic AIF3 counterpart from disk abalone (*Haliotis discus discus*) deciphering its transcriptional modulation by induced pathogenic stress

Don Anushka Sandaruwan Elvitigala [a, b], R.G.P.T. Jayasooriya [a], Ilson whang [b], Jehee Lee [a, b, *]

[a] Department of Marine Life Sciences, School of Marine Biomedical Sciences, Jeju National University, Jeju Self-Governing Province 690-756, Republic of Korea

[b] Fish Vaccine Development Center, Jeju National University, Jeju Special Self-Governing Province 690-756, Republic of Korea

ARTICLE INFO

Article history:
Received 10 July 2015
Received in revised form
2 October 2015
Accepted 5 October 2015
Available online 9 October 2015

Keywords:
Disk abalone
Apoptosis inducing factor 3
Apoptotic activity
Immune stimulation
Transcriptional modulation

ABSTRACT

Apoptosis inducing factor (AIF) is a flavoprotein that is involved in oxidative phosphorylation and induces apoptosis in eukaryotic cells. There are three isozymes of AIF that have been identified to date, designated as AIF1, AIF2, and AIF3; the human AIF3 is also known as an AIF-like protein (AIFL). This study aimed to identify and characterize a homologue of AIF3 from disk abalone (AbAIF3) that belongs to the phylum Mollusca. The open reading frame (ORF) of *AbAIF3* is 1749 base pairs (bp) in length and encodes a protein of 583 amino acids, with a predicted molecular mass of 63.14 kDa. Based on our *in-silico* analysis, the AbAIF3 protein harbored the typical domain architecture as that of the known AIF family proteins, consisting of N-terminal Rieske and pyridine nucleotide-disulphide oxidoreductase domain. Comparative protein sequence analysis confirmed that AbAIF3 is a homolog of AIF3. Moreover, our phylogenetic analysis revealed that AbAIF3 had a close evolutionary relationship with the molluscan counterparts. Interestingly, AbAIF3 was shown to induce apoptosis in HEK293T cells using transfection assays followed by flow cytometric analysis. In addition, we found that *AbAIF3* mRNA expression was ubiquitous in physiologically important tissues, and significantly modulated upon experimental immune stimulations in hemocytes. Collectively, our study illustrates the indispensable role of AbAIF3 in inducing apoptosis in disk abalones, which in turn might be involved in hosts' immune defense mechanisms against microbial infections.

1. Introduction

Apoptosis is a crucial cellular process that occurs in animal cells under physiological conditions or during an infection. Apoptosis is a form of programmed cell death that is characterized by morphological changes, such as cell shrinkage, apoptotic body formation, and chromatin condensation [1]. Apoptosis is prominently involved in regulatory processes in immune cells, including maturation and homeostasis [2]. It also plays a role in eliminating infected cells from the host organism after interacting with the host immune defenses [3,4]. In general, apoptosis can be induced via two basic pathways: intrinsic and extrinsic. In the intrinsic pathway, mitochondria-mediated apoptosis occurs due to the release of different apoptotic proteins, including cytochrome C, endonuclease G, and apoptosis inducing factor (AIF) [5]. Even though some differences on apoptotic mechanisms orchestrating in invertebrates with those functioning in vertebrates were reported, most of them are almost well conserved in invertebrate linages. As reported for vertebrates, apoptosis in invertebrates also known to involve in host immune responses. For instance, in mollusks, induction or inhibition of apoptosis in response to pathogen or parasitic infections was reported previously. In one study, apoptosis was detected to be induced by phagocytosis of live or killed marine bacteria, *Planococcus citraeus* in hemocytes of Pacifc oyster, as a result of oxidative damage on the hemocytes during reactive oxygen species (ROS) mediated bacterial eradication [6]. Moreover, Symbiotic bacteria (*Vibrio* spp.) also could elevate apoptosis in host

* Corresponding author. Marine Molecular Genetics Lab, Department of Marine Life Sciences, College of Ocean Science, Jeju National University, 66 Jejudaehakno, Ara-Dong, Jeju, 690-756, Republic of Korea.
E-mail address: jehee@jejunu.ac.kr (J. Lee).

http://dx.doi.org/10.1016/j.fsi.2015.10.006
1050-4648/

cells of some cephalopods [7]. Rapid induction of apoptosis in hemocytes in response to the parasitic infection caused by *Perkinsus marinus* was also reported from *P. marinus* resistant Pacific oyster [8]. On the other hand, apoptosis levels in hemocytes were shown to be markedly reduced from 50% to ~10% in oysters infected by some parasites including *P. marinus* and *Haplosporidium nelson* [9].

AIF is a flavoprotein, which acts as a NADH oxidase under physiological conditions that involves in oxidative phosphorylation [10–12], as well as in caspase-independent apoptosis [13]. According to the phylogenetic analysis, AIF (currently known as, AIF1) is categorized within a larger family of eukaryotic proteins that are found in animals and fungi. This family of proteins consists of structurally and functionally related proteins, such as mitochondrion associated inducer of death (AMID, also known as AIF2) and the AIF-like (AIFL) protein (also known as AIF3) [14–17]. However, the aforementioned AIF1, AIF2, and AIF3 are now recognized as AIF isozymes.

In humans, AIF is expressed as a precursor protein with two N-terminal mitochondrial localization signal peptides (MLSs) (67 kDa) and localizes to the mitochondrial intermembrane space [18–20]. Upon export to mitochondria, the precursor AIF undergoes calpain or cathepsin mediated cleavage [21,22] to remove the MLS and become a mature protein (57 kDa) that only harbors a FAD binding domain, a NADH binding domain, and a C-terminal domain [19]. The FAD binding domain and the NADH binding domain represents the oxidoreductase portion of the mature AIF [10], whereas the C-terminal domain is important for its pro-apoptotic function [23]. When AIF is released from the mitochondria, it is translocated to the nucleus where it triggers chromatin condensation and large scale DNA fragmentation [18]. Besides its apoptotic function, AIFs also plays a role in lethal responses to excitotoxins, hypoxia-ischemia, growth factor deprivation, mitochondrial metabolism, and redox control [24]. Interestingly, AIF was also found to inhibit chemical stress-mediated apoptosis in human colon cancer cells [25].

Three basic isoforms of AIF1 have been identified in humans, designating AIF-exB [26], AIFsh [23], and AIFsh2 [27]. Intriguingly, AIFsh lacks an N-terminal oxidoreductase domain, however, it can induce prominent apoptotic characteristics like AIF1, which suggests that the oxidoreductase portion of the protein is not required for the apoptotic function of AIFs. On the other hand, AIFsh2 was found to lack the C-terminal domain of AIF, hence, it does not show the same pro-apoptotic activities as AIF. This result confirms that the C-terminal domain of AIF is essential and sufficient to elicit AIF-mediated nuclear apoptosis in cells. However, some of the previous reports implied that the oxidoreductase part of AIF1 might be involved in caspase-independent apoptosis through the production of reactive oxygen species [10,25,28]. According to these previous reports, AIF has an indispensable role in animal physiology, which was confirmed using experimental studies on AIF orthologues from model organisms, including *Saccharomyces cerevisiae, Caenorhabditis elegans, Drosophila melanogaster,* and mice [24]. Nevertheless, there are few reports characterizing AIFs from other organisms in different taxonomic lineages. Thus, the identification and functional characterization of AIFs from different taxonomic groups is a necessity in order to expand our understanding of animal AIFs.

Abalones are marine gastropods, which are highly sought after aqua-crops in the worldwide shellfish aquaculture industry, especially in the Asia Pacific. However, some of these species are at a risk of extinction due to overconsumption and the acidification of oceans from anthropogenic carbon dioxide [29]. Moreover, these creatures are highly sensitive to a wide range of environmental conditions that impart negative effects on their survival and growth, and make them more susceptible to pathogenic infections and toxicants. Thus, these mollusks are important bio-indicators in the marine eco-system [30]. For instance, abalones can be infected by numerous bacteria [31,32], virus [33], and parasites [34]. Therefore, gaining insight into the host defense mechanisms of abalones at molecular level is an important strategy in order to prevent their mass mortality, especially as it relates to their role in aqua-farming.

In this study, we identified and characterized an AIF3 homologue from disk abalone (*Haliotis discus discus*) and analyzed its transcriptional modulation in response to pathogen-derived mitogens. To our knowledge, this is the first report describing the role of AIF3 in mollusks. In addition, we investigated AIF3 expression patterns in different tissues from healthy abalones. Moreover, we used a cellular approach to analyze the pro-apoptotic activity of this novel AIF homologue *in vitro.*

2. Materials and methods

2.1. Identification and in-silico characterization

We have established a cDNA database of disk abalone using the Roche 454 Genome sequencer FLX system (GS-FLX™) [35]. Briefly, after total RNA extraction from gills, mantel, digestive tract, hepatopancreas, head and muscle tissues of healthy abalones using the TRI Reagent™ kit (Sigma–Aldrich, Missouri, USA), the isolated RNA was purified using the FastTrack® 2.0 mRNA isolation kit (Invitrogen, USA). Thereafter, we generated a cDNA library, which was normalized using the Creator™ SMART™ cDNA library construction kit (Clontech, USA) and a Trimmer cDNA normalization kit (Evrogen, Russia), respectively. The contig sequences of the established database were then analyzed using the Basic Local Alignment Search Tool (BLAST) algorithm (http://blast.ncbi.nlm.nih.gov/Blast.cgi), which allowed for the identification of homologue sequence to *Pomacea canaliculata* AIF3 (AbAIF3) with a 66% sequence identity, 70% quarry coverage and 0.0 E-value. Subsequently, the complete putative open reading frame (ORF) was identified and the corresponding amino acid sequence was derived using the DNAsist 2.2 (version 3.0) software. Characteristic domain signatures of the AbAIF3 protein were predicted using the NCBI-CDD server (http://www.ncbi.nlm.nih.gov/Structure/cdd), while the MLS was attempted to identify using the TargetP 1.1 Server (http://www.cbs.dtu.dk/services/TargetP) and PSORT sever, separately (http://psort.hgc.jp/). Several physicochemical properties of the protein were determined with the ExPASy protParam tool (http://web.expasy.org/protparam). Moreover, sequence comparisons at the protein level were performed using multiple sequence alignments and pairwise sequence alignments with ClustalW2 [36] and the MatGAT software [37], respectively. The evolutionary relationship of AbAIF3 to other known homologues were evaluated by generating phylogenetic reconstructions using the Molecular Evolutionary Genetics Analysis (MEGA) software version 5 [38], followed by the Neighbor-joining method with the support of 1000 bootstrap replications.

2.2. Preparation of the recombinant vector construct

The complete coding region of *AbAIF3* was PCR amplified using the corresponding cloning primer pair (AbAIF3-F and AbAIF3-R, Table 1), which harbored restriction enzyme sites for *Eco*RI and *Xho*I, respectively. PCR was carried out in a TaKaRa thermal cycler (TaKaRa, Otsu, Shiga, Japan) in a total volume of 50 μL, containing 5 units (U) of TaKaRa ExTaq polymerase, 5 μL of 10 × TaKaRa ExTaq buffer, 4 μL of 2.5 mM dNTPs, 80 ng of template, and 40 pmol of each primer (Table 1). PCR was performed under the following conditions: initial denaturation at 94 °C for 3 min, followed by 35

Table 1
Primers used in this study.

Name	Purpose	Sequence (5′ → 3′)
AbAIF3-F	PCR amplification of *AbAIF3* ORF for cloning (*Eco*RI)	GAGAGAgaattcATGATGGGGAAGAAACACTCCAAGTTCGA
AbAIF3-R	PCR amplification of *AbAIF3* ORF for cloning (Xho*I*)	GAGAGActcgagTCAGAACTTCTGAAGTCGACTTGTCCAC
AbAIF3-qF	qPCR analysis of *AbAIF3*	TATGGACATAAAGCCGGAGGCCAT
AbAIF3-qR	qPCR analysis of *AbAIF3*	GCTGAACTTCACAGATTTGCCGCT
Ab-Rp-F	qPCR analysis of abalone ribosomal protein L5 gene	TCACCAACAAGGACATCATTTGTC
Ab-Rp-R	qPCR analysis of abalone ribosomal protein L5 gene	CAGGAGGAGTCCAGTGCAGTATG

cycles of 94 °C for 30 s, 57 °C for 30 s, and 72 °C for 1.5 min, with a final extension at 72 °C for 5 min. The PCR product (~1.7 kbp) and the pCDNA3.1/His-C plasmid (4 μg) were digested with *EcoRI* and *XhoI* (TaKaRa, Japan), according to the manufacturer's instructions and resolved on a 1% agarose gel. Thereafter, the corresponding DNA bands were excised, and purified using the Accuprep™ gel purification kit (Bioneer Co. Korea). The digested vector (40 ng) and PCR product (40 ng) were ligated using Mighty Mix (5.0 μL; TaKaRa, Japan) at 4 °C overnight. The ligated product was then transformed into *Escherichia coli* DH5α cells and sequenced. The sequence verified recombinant vector (pCDNA-AbAIF3) was used for the subsequent transfection assay.

2.3. Cell culture and transfection assay

Human embryonic kidney 293T (HEK293T) cells were grown in Dulbecco Modified Eagle Medium (DMEM- WELGENE-Korea) supplemented with 10% fetal bovine serum (FBS) and maintained at 37 °C in 5% CO_2. The prepared pCDNA-AbAIF3 recombinant construct was transfected into HEK293T cells using the FuGENE®6 transfection reagent (Promega, USA), according to manufacturer's instructions.

2.4. Cell viability assay

HEK293T cells were seeded in 24-well plates and transfected with the target plasmid (AbAIF3-pCDNA − 1 μg) as mentioned in Section 2.3., after the cells reach ~80% confluency. Cells were then subjected to standard colorimetric MTT assay. Briefly, HEK293T cells were treated with 50 μL of MTT reagent [2 mg/mL in phosphate buffered saline (PBS)] 24 h post-transfection and incubated for 3 h. Thereafter, the plate was centrifuged for 10 min at 2000 rpm and the supernatants were aspirated. Subsequently, the remaining formazan crystals in each well were dissolved in di-methyl sulfoxide (DMSO) and the optical density (OD) was measured at 540 nm in order to quantify the amount of formazan in the final solution. Finally, the viability of transfected, mock controls (empty pCDNA3.1/HisC) or transfection controls (no vector) was determined by comparing these values to that of the un-transfected control, which was set at 100% viability. These assays were carried out in triplicate to ensure the credibility of the results.

2.5. Determining the induction of apoptosis

To determine the potential apoptotic activity of AbAIF3, HEK293T cells were transfected with the AbAIF3-pCDNA construct and the cells were analyzed by flow cytometery. Briefly, HEK293K cells were seeded in 6-well plates and transfected with 6 μg of AbAIF3-pCDNA or pCDNA 3.1.His-C empty vector (mock control experiment), as described earlier. The cells were analyzed with a FACSCalibur flow cytometer (Becton Dickenson; San Jose, CA) at 24 h post-transfection after staining with annexin-V FITC (R&D systems). Herein, cells were initially fixed in 1 U/mL of RNaseA (DNase-free) and 10 μg/mL of propidium iodide (Sigma) overnight in dark at room temperature. The cells were then washed with PBS prior to the annexin-V staining. In addition to the mock experiment, two other control experiments were carried out by transfecting HEK293T cells in the absence of vector (transfection control) or in the absence of treatment (un-transfected control). All of the experiments were triplicated to ensure the credibility of outcomes.

2.6. Shellfish rearing and tissue extraction

Healthy abalones (~50 g) were purchased from the Youngsoo commercial abalone farm in Jeju Island, Republic of Korea. Abalones were reared at the Marine Science institute of Jeju National University, in 250 L flat-bottom tanks filled with sand–filtered seawater (salinity - 34 ± 0.6 psu and temperature - 20 ± 1 °C) with aeration, with 30 abalones per tank. Animals were acclimatized for one week prior to experimentation and were fed with fresh marine seaweed (*Undaria pinnatifida*). Four healthy animals were sacrificed to collect the hemolymph from the pericardial cavities using sterilized syringes and the samples were immediately centrifuged (3000 × g at 4 °C for 10 min) to harvest the hemocytes. Tissues from the adductor muscle, mantle, gill, hepatopancreas, digestive tract, and brain were collected from four animals, frozen in liquid nitrogen and stored at −80 °C for future use.

2.7. Immune stimulation experiment

Healthy abalones with an average size of 8 cm were stimulated with pathogen-derived chemicals. A group of 30 abalones were intramuscularly injected with 100 μL (500 μg/animal) of lipopolysaccharide (LPS) in saline, which equates to a dose of approximately 10 mg/kg (*E. coli* 0127:B8; Sigma–Aldrich). Another group (30 animals) was injected with 100 μL (10 μg/μL) of polyinosinic:polycytidylic acid (poly I:C) (Sigma–Aldrich) in saline. Two additional groups of abalones served as uninjected control (10 abalones) and injected control (30 abalones), where the latter was injected with the equal amounts of saline. Hemolymphs were extracted and the hemocytes were collected from both the control groups and the challenged groups at respective time points (described in Section 2.5). Total RNA was extracted from the corresponding tissues and cells from at least four animals and used for cDNA synthesis.

2.8. RNA extraction and cDNA synthesis

Total RNA was extracted with Tri-Reagent™ (Sigma–Aldrich) from abalone adductor muscle, mantle, gill, hemocytes, digestive tract, hepatopancreas, and brain from four abalones, as well as from the collected hemocytes of immune-stimulated abalones (4 animals at each time point). Concentration was determined by measuring the OD at 260 nm in a UV spectrophotometer (Bio-Rad, USA). Purified RNA samples were diluted to 1 μg/μL and subjected to cDNA synthesis through reverse transcription PCR using the PrimeScript™ cDNA Synthesis Kit (TaKaRa), according to the manufacturer's instructions. Finally, newly synthesized cDNA was

diluted 40-fold (800 μL total) before being stored at −20 °C until further analysis.

2.9. Quantification of mRNA expression

Basal transcript levels in extracted tissues from healthy abalones and temporal transcriptional modulation in hemocytes from immune-challenged animals were evaluated by quantitative PCR (qPCR) using the corresponding cDNAs as a template. Reactions were performed using the Dice™ (Real Time System TP800; TaKaRa, Japan) thermal cycler in a 10 μL reaction volume that contained 3 μL of diluted cDNA, 5 μL of 2 × TaKaRa Ex-Taq™ SYBR Green Premix, 0.4 μL of each primer (AbAIF3-qF and AbAIF3-qR) (Table 1) and 1.6 μL of nuclease free H_2O. qPCR was carried out under the following conditions: 95 °C for 10 s, then 40 cycles of 5 s at 95 °C, 10 s at 58 °C and 20 s at 72 °C, and a final cycle of 95 °C for 15 s, 60 °C for 30 s and 95 °C for 15 s. The baseline was set automatically by the Dice™ thermal cycler Real Time System Software (Version 2.00) (TaKaRa, Japan). AbAIF3 expression was determined by the Livak ($2^{-\Delta\Delta Ct}$) method [39]. The same qPCR cycle profile was used for the internal control gene, abalone ribosomal protein L5 gene (GenBank ID: EF103443), using corresponding primers (Table 1) which did not show any significant expressional variation within each tissue under provided experimental conditions. Assay was employed according to the essential MIQE guidelines [40]. Expression levels were analyzed in triplicated qPCR assays, and all of the data was presented as relative mRNA expression by calculating the mean ± standard deviation (SD). The transcript levels that were detected following each stimulant were compared with the expression levels of the internal reference gene, and further normalized to the expression levels of the corresponding saline-injected controls at each time point post-injection. In addition, the relative transcript level of an un-injected control (0 h) group was defined as the basal expression level in each experiment. We used a two-tailed unpaired t-test to determine the statistical significance ($P < 0.05$) between each experimental group and the un-injected control group.

3. Results and discussion

3.1. Sequence profiles and comparison

We identified a cDNA sequence of 2222 bp, which showed homology to the known AIF3 homologues and harbored a 1752 bp open reading frame (ORF) that encoded for a 583 amino acid sequence with predicted molecular mass of 63.14 kDa and a theoretical isoelectric point of 6.55. Sequence details were deposited in the NCBI-GenBank sequence database under the accession number KP973857. As indicated by the outcomes of our *in silico* analysis, AbAIF3 showed the characteristic domain architecture of known AIF3s, including the N-terminal Rieske, the 2Fe–2S cluster binding domain (residues 59–153) harboring (2Fe–2S) cluster binding sites (residues 98, 100, 101, 117, 120 and 122) and the pyridine nucleotide-disulphide oxidoreductase signature (Pyr-redox; residues 318–399) (Fig. 1). However, we could not identify a MLS sequence at the N-terminal region of the protein during our bioinformatic analysis, which is a commonly identified feature of vertebrate AIF homologues. As expected, in a pairwise sequence comparison with its known homologues, AbAIF3 had the highest sequence identity (60.8%) and similarity (72%) with its molluscan counterpart, *Pomacea canaliculata* (apple snail) (Table 2). Intriguingly, AbAIF3 showed a greater degree of sequence identity with vertebrate AIF3s than the other invertebrate homologues that were analyzed during comparison, such as *Crassostrea gigas* (Pacific oyster) and *Bactrocera dorsalis* (Oriental fruit fly) which deserves

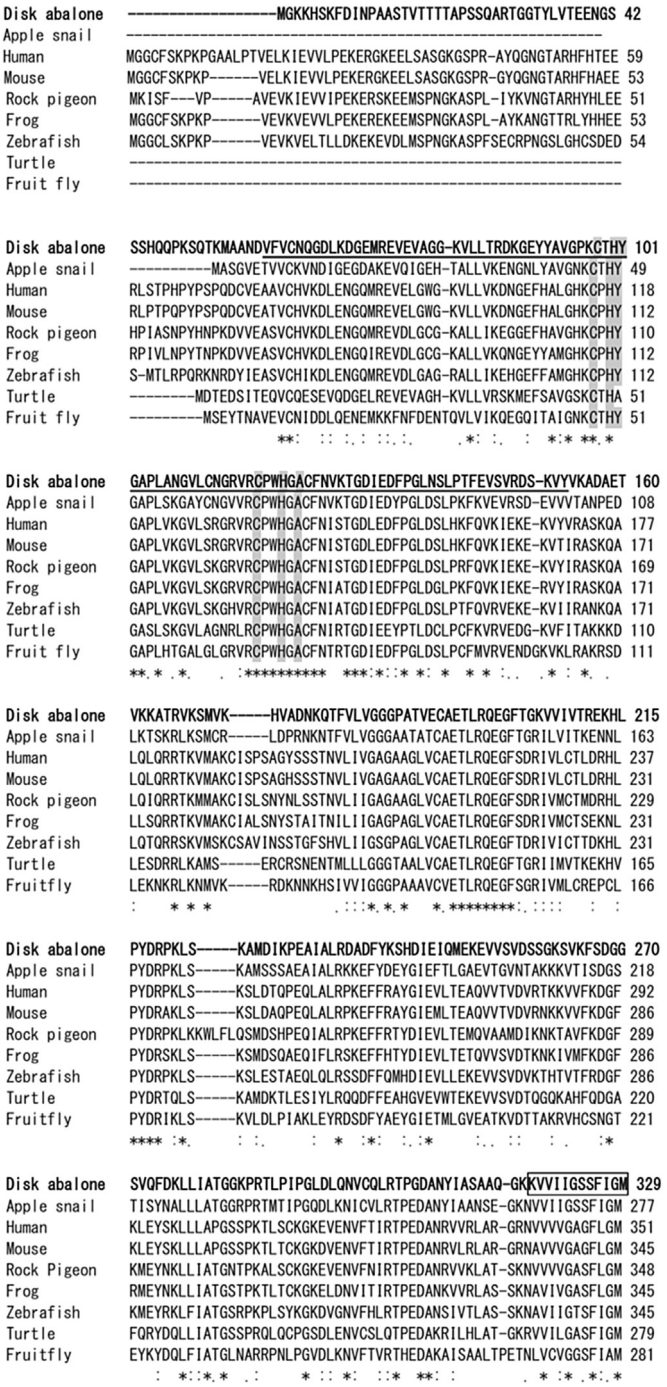

Fig. 1. Multiple sequence alignment of AbAIF3 with some of the known AIF3 counterparts. Rieseke domain signature and Pyr-redox signature was underlined and boxed on AbAIF3 sequence, respectively. Conserved (2Fe-2s) cluster binding sites were shaded in gray color. Completely and partially conserved residues among the sequences were indicated by (*) and (.) or (:) signs.

further investigations. However, this comparison validates that AbAIF3 shares more sequence identity with AIF3 than the rest of the AIF homologues (AIF1 and 2). According to our multiple sequence alignment, the predicted 2Fe–2S cluster binding sites that were identified in AbAIF3 were highly conserved amongst the other homologues that were used in the analysis, prefiguring the functional homology of AbAIF3 with known AIF3 counterparts (Fig. 1).

Fig. 1. (*continued*).

3.2. Phylogenic relationships

According to our phylogenetic reconstruction, the three types of AIFs clustered in closely-related albeit separate clades where AbAIF3 was grouped with AIF3 homologues, as expected (Fig. 2). Moreover, AbAIF3 was clustered with the apple snail AIF3 with a satisfactory bootstrap support (63) forming a sub-clade, reinforcing the observed sequence identity between these homologues. However, the molluscan AIF3 homologue from the pacific oyster diverged from the aforementioned sub-clade, reflecting an evolutionary distinct relationship with the other two molluscan homologues. Nevertheless, all three molluscan AIF3 homologues were grouped together in a separate clade, illustrating that they shared an ancestral origin that diverged from the clade of vertebrate AIF3s (Fig. 2). Intriguingly, molluscan AIF3 homologues showed a relatively closer evolutionary relationship with vertebrate AIF3s than insect AIF3s (fruit fly). On the other hand, some of the insect homologues of AIF1 (termites and ants) shared a closer phylogenetic relationship with vertebrates than its invertebrate homologues (pacific oyster AIF1). Collectively, these data clearly demonstrate that AbAIF3 is a member of the AIF3 family and is more closely related to its vertebrate homologues.

3.3. Apoptotic property of AbAIF3

Cell viability of HEK293T cells after transfection with AbAIF3-pCDNA was measured by MTT assay. Expression of AbAIF3 at mRNA level in HEK293T cells were confirmed by semi quantitative PCR using AbAIF3qF and AbAIF3qR primer pair (Table 1; data not shown), using human beta actin gene as an internal reference (Gene bank ID: DQ407611). According to the viability percentage that was determined relative to the un-transfected control, recombinant AbAIF3-pCDNA vector transfected cells showed significantly lower (63%) viability (Fig. 3). As expected, the cells used in the mock control experiment or transfection control experiment did not demonstrate any significant viability difference (100% and 94% viability, respectively) than that of the un-transfected controls, which confirms that the transfection procedure and vector backbone did not affect cell viability (Fig. 3). Collectively, the data suggests that the AbAIF3 protein is expressed in live animal cells and can potentially induce apoptosis.

After transfecting the AbAIF3-pCDNA recombinant vector into HEK293T cells, the cells were analyzed by flow cytometry after staining with annexin-V. Our results showed that the cells transfected with the recombinant vector had substantial annexin V staining (44.7 ± 2.3% out of total cell population) compared to the controls, demonstrating that a significant portion of HEK293T might have undergone apoptosis (Fig. 4A – upper panel and Fig. 4B), since annexin V can easily bind phosphtisylserines which are commonly expressed on surface of cells undergoing apoptosis [41]. As expected, the cells in the mock control experiments and transfection control experiments were stained by annexin-V, similar to the un-transfected control experiments (16.05 ± 1.5%, 17.81 ± 1.4% and 17.29 ± 1.2%, out of total cell population, respectively). These data corroborate that the transfection procedure and vector backbone did not significantly alter cell viability. When we use our light microscope to examine the cellular morphology before staining with annexin V, as expected the cells treated with AbAIF3-pCDNA recombinant vector displayed decreased cell number with some apoptotic shrinkage compared to the control experiments, reinforcing the outcomes of our flowcytometric analysis (Fig. 4A – lower panel). Overall, this experimental evidence clearly confirms that AbAIF3 plausibly induce apoptosis in live animal cells.

3.4. Tissue specific mRNA expression

As detected by qPCR, *AbAIF3* mRNA was found to be ubiquitously expressed in all the examined tissues, although the most pronounced expression was observed in digestive tract tissues. Universal expression of *AbAIF3* in physiologically important tissues suggests that it has an important role in abalone physiology since AIF3s are known to be involved in cellular apoptosis, mitochondrial metabolism and redox balance in animals (Fig. 5). Similarly, human AIFL (AIF3) was reported to be constitutively expressed in multiple and physiologically important organs, including the brain, colon, heart, kidney, liver, lung, muscle, pancreases, placenta and small intestine [17]. Generally, the digestive gland of aquatic, as well as terrestrial mollusks are involved in the accumulation and detoxification events of the toxicants (i.e., metals), which in turn trigger apoptosis [42]. AIFs are also known to play a role in lethal responses to excitotoxins [24]. Therefore, it is not unlikely to expect pronounced expression of AIFs, including AIF3, in the digestive tract of abalones.

3.5. Transcriptional responses to the immune stimulation

In order to evaluate the apoptotic potential in abalones in response to pathogenic stress, expressional modulation of *AbAIF3*

Table 2
Percentage identity and similarity of AbAIF3 shared with known AIF counterparts.

Organism	Protein	Accession number	Amino acids	Identity (%)	Similarity (%)
1. *Pomacea canaliculata* (Apple snail)	AIF3	AFQ23946	532	60.8	72
2. *Danio rerio* (Zebrafish)	AIF3	NP001121885	599	47.7	66.4
3. Chelonia mydas (Green sea turtle)	AIF3	EMP37830	530	47.3	64.3
4. *Homo sapiens* (Human)	AIF3	NP001139760	604	47	66.7
5. *Xenopus laevis* (African clawed frog)	AIF3	NP001081029	605	46.2	65.8
6. *Bos taurus* (Bovine)	AIF3	NP001039746	598	45.8	66.1
7. *Columba livia* (Rock pigeon)	AIF3	EMC76958	601	45.8	66.1
8. *Mus musculus* (Mouse)	AIF3	NP001277999	605	45.7	65.3
9. *Crassostrea gigas* (Pacific oyster)	AIF3	EKC20321	890	40.1	50.1
10. *Ceratitis capitata* (Mediterranean fruit fly)	AIF3	JAB99107	545	38.6	58.5
11. *Bactrocera dorsalis* (Oriental fruit fly)	AIF3	JAC46086	660	36.9	54.7
12. *Mus musculus* (Mouse)	AIF1	NP036149	612	23	41.2
13. *Homo sapiens* (Human)	AIF1	NP004199	613	22.8	40.5
14. *Gallus gallus* (Chicken)	AIF1	NP001007491	591	22.4	40.4
15. *Danio rerio* (Zebrafish)	AIF1	NP956396	613	22	40.6
16. *Harpegnathos saltator* (Ant)	AIF1	EFN81142	655	21.2	40.3
17. *Drosophila melanogaster* (Fruit fly)	AIF1-A	NP608649	674	21	37.7
18. *Ascaris suum* (Pig roundworm)	AIF1	ADY42032	717	20.6	36
19. *Zootermopsis nevadensis* (Dampwood termites)	AIF1	KDR07550	719	20.3	36.3
20. *Crassostrea gigas* (Pacific oyster)	AIF1	EKC36189	543	19.8	39.5
21. *Drosophila melanogaster* (Fruit fly)	AIF1-B	NP722765	739	19.8	35.3
22. *Drosophila melanogaster* (Fruit fly)	AIF1-C	NP001259907	738	19.7	35.2
23. *Xenopus laevis* (Frog)	AIF2	NP001091397	374	18.8	31
24. *Ictalurus punctatus* (Channel catfish)	AIF2	AHH43077	373	18.2	31.6
25. *Danio rerio* (Zebrafish)	AIF2	NP001186939	373	18	30.5
26. *Mus musculus* (Mouse)	AIF2	NP835159	373	16.9	30
27. *Homo sapiens* (Human)	AIF2	NP001185625	373	16.4	31.9

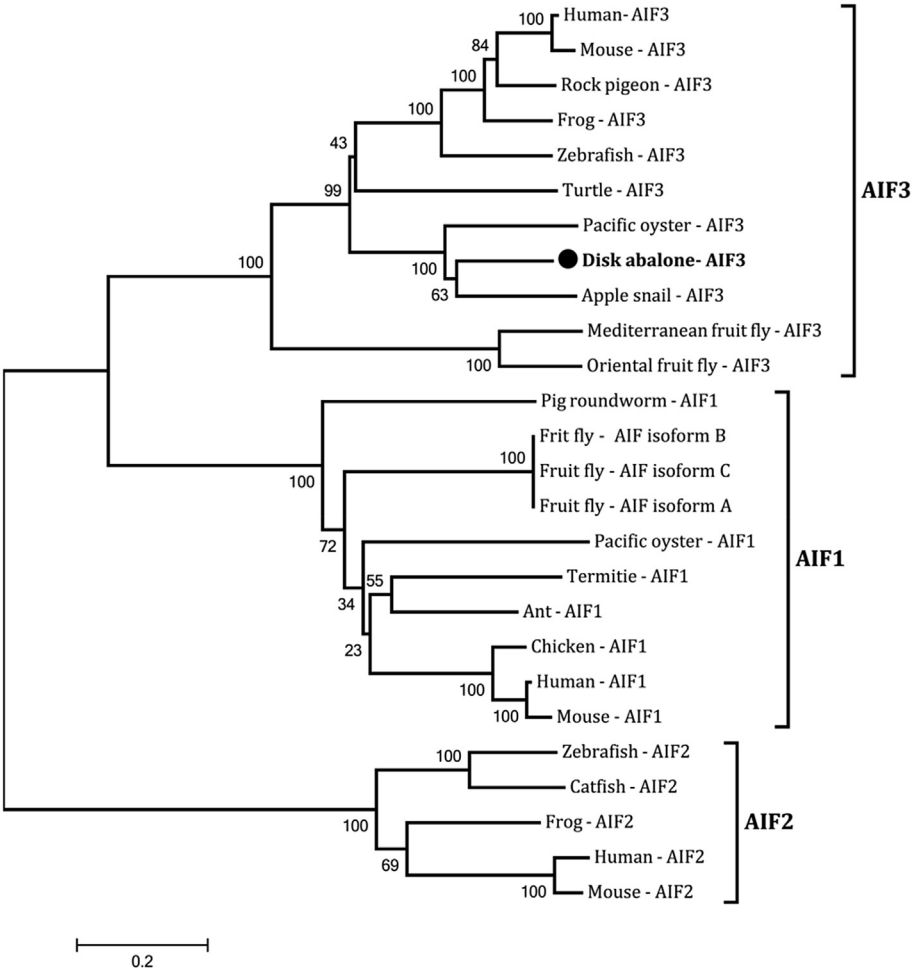

Fig. 2. Phylogenetic reconstruction of AbAIF3 generated using different vertebrate and invertebrate AIF counterparts. The evolutionary relationship was evaluated using MEGA 5.0 software, following neighbor-joining platform, based on ClustalW protein sequence alignment. Corresponding bootstrap values are indicated on each branch of the tree. NCBI GenBank accession numbers of each AIF counterpart used in the construction are listed in Table 2.

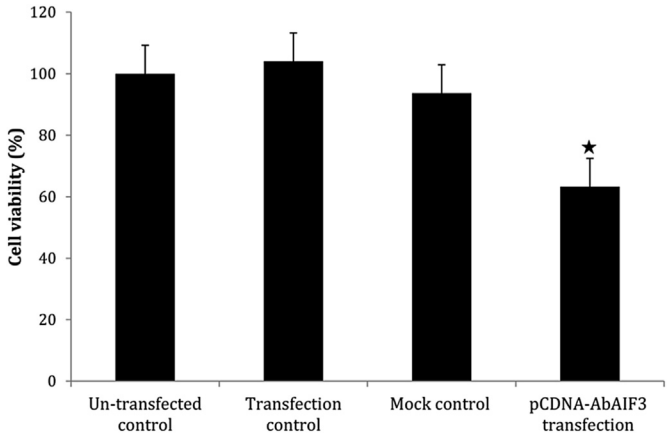

Fig. 3. Effect of AbAIF3-pCDNA transfection on viability of HEK293T cells as determined by standard MTT assay. Data illustrate respective experiment. Error bars represent the SD (n = 3). Viability (%) significantly different ($P < 0.05$) from negative control was denoted by (★).

was analyzed in hemocytes from abalones after being treated with poly I:C or LPS so as to emulate a viral or bacterial infection, respectively. Hemocytes in molluscs play a significant role in host innate immune responses through their phagocytic and antibacterial activities, which in turn can trigger hemocytic apoptosis as a subsequent defense response [6]. Thus, hemocytes were selectively used to evaluate the transcriptional responses against the induced pathogen stress.

After treating with Poly I:C, which is a well-known synthetic viral double stranded RNA analog, *AbAIF3* transcription was significantly up-regulated from its basal level in the early phases of the experiment [3 h, 6 h, 12 h and 24 h post injection (p.i.)] with marked fold increases (~8 fold) at 6 h p.i. (Fig. 6A). However, thereafter the transcript level was down-regulated at 48 h p.i. and returned to its basal level at 72 h p.i. Apoptosis is considered one of the basic host immune defense mechanisms against viral infections and are trigged by the recognition of the infected agents, most likely sensing through the pathogen associated molecular patterns (PAMPs) by relevant pattern recognition receptors [43]. Thus, the elevation of *AbAIF3* basal transcription in response to Poly I:C treatment suggests that it can induce apoptosis in abalone hemocytes [44]. However, late phase down-regulation of *AbAIF3* expression may be a representation of a mRNA turnover event [45] in hemocytes in response to the changes of the cellular environment due to the poly I:C treatment, which was counterbalanced at 72 h p.i. and reached basal mRNA levels.

Upon the treatment of the well-known bacterial endotoxin LPS, *AbAIF3* expression was significantly up-regulated at 12 h p.i., though significantly down-regulated at early (3 h p.i) and late

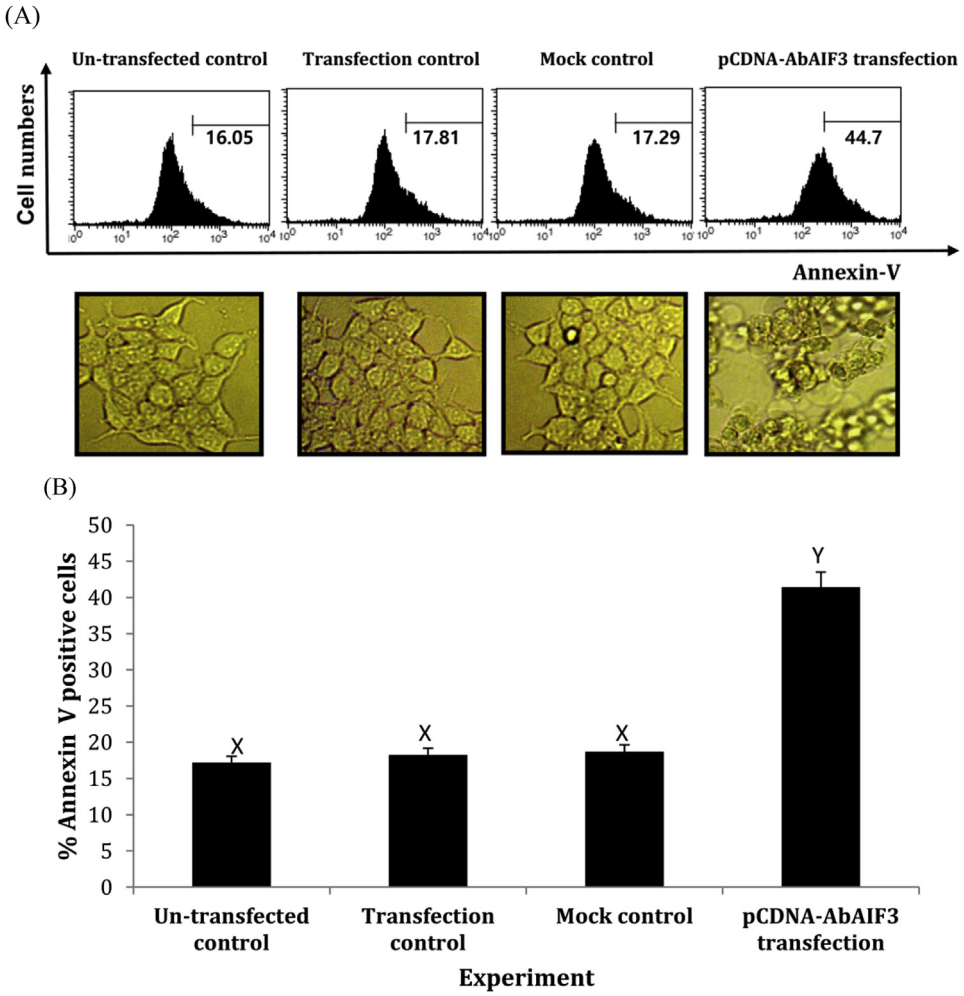

Fig. 4. Flow cytometric analysis of apoptosis induction in HEK293T cells by AbAIF3. (A) Annexin-V stained cell population was measured in each indicated experiment using flow cytometery (upper panel) and morphology of the cells were examined by light microscopy (400 x) (lower panel) before Annexin V staining. Assay was triplicated and affirmed the credibility of the outcomes. (B). Percentage of Annexin V stained cells out of total cell population, corresponding to the each experiment as detected by flowcytometery. Different letters represent statistically different staining levels (n = 3; $P < 0.05$).

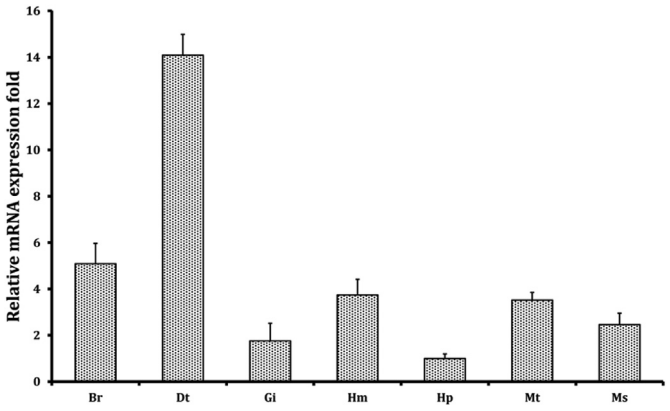

Fig. 5. Tissue-specific mRNA expression of *AbAIF3*. Br-brain, Dt-digestive tract, Gi – gill, Hm – hemocytes, Hp – Hepatopancreas, Mt – Mantle and Ms –adductor muscle. Expression fold-changes of mRNA expression detected by qPCR and evaluated by the $2^{-\Delta\Delta CT}$ method using disk abalone ribosomal protein L5 gene as the reference gene are presented as relative to that in Hp. Error bars represent the SD (n = 3).

phases (48 h p.i.) of the experiment (Fig. 6B). Overall, transcript levels of *AbAIF3* fluctuated in response to LPS throughout the time course. Production ROS is a primary and immediate immune response in animals infected with bacteria, which can be triggered through PAMPs [46,47]. Nevertheless, AIFs appear to play an important role in scavenging ROS to maintain the redox homeostasis in cellular environments [11,48]. Therefore, the initial repression in *AbAIF3* expression may likely be an immune response that maintains a high ROS level in cells after sensing LPS. However, when *AbAIF3* expression was elevated, the excessive levels of ROS may be counterbalanced by the expressed AbAIF3 in the cells. On the other hand, the detected up-regulation may represent a potential AbAIF3 mediated apoptotic process, since apoptosis can be induced by recognizing LPS-like PAMPs through PRRs, like TLRs [49]. However, similar to the poly I:C treatment, the late phase down-regulation may reflect a mRNA decay due to the effect of the endotoxin in the cells. Altogether, expressional modulation of *AbAIF* upon the treatment with two different chemicals suggests that its putative significance in host innate immune responses against microbial invasions, which deserves further investigations.

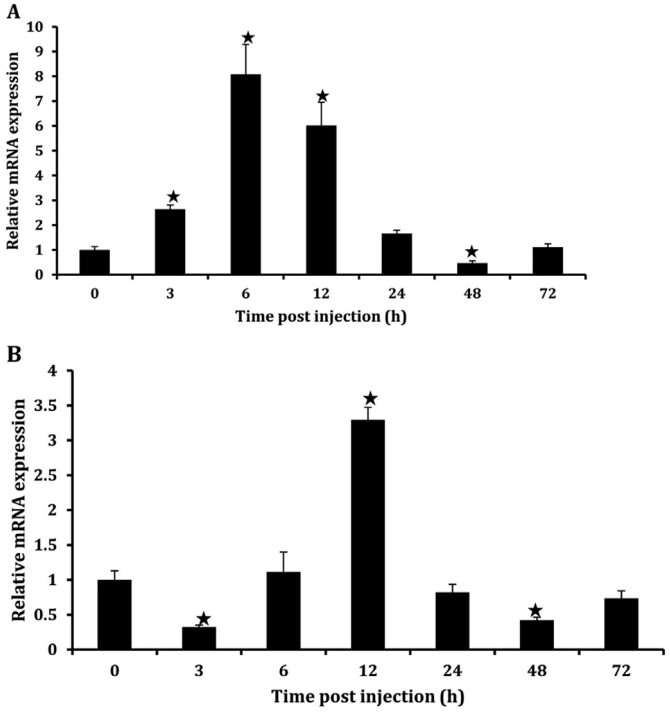

Fig. 6. Temporal modulation of *AbAIF3* transcription in hemocytes upon immune stimulation with (A) lipopolysaccharides (LPS) and (B) poly I:C, as measured using qPCR. The relative expression was calculated using the $2^{-\Delta\Delta CT}$ method. Disk abalone ribosomal protein L5 gene was used as the reference gene, further normalizing to the corresponding saline-injected controls at each time point. The relative fold-change in expression at 0 h post-injection was used as the baseline. Error bars represent SD (n = 3); expression levels significantly different from that of un-injected control were denoted using ★.

4. Conclusion

A homologue of AIF3 (AIFL) was identified from disk abalone and characterized at molecular level. Our basic bioinformatic analysis ascertains that AbAIF3 is a member of AIF family by detecting important characteristic signatures of AIF family. Comparative sequence analysis further supports the notion that AbAIF3 is homologous to other known AIF3s. Moreover, it has a close evolutionary relationship with molluscan homologues, followed by vertebrate homologues. Using a cellular approach, *in vitro* apoptotic properties of AbAIF3 were confirmed by using flow cytometry. In addition, ubiquitous tissue-specific basal expression of AbAIF3 was detected using qPCR, which further demonstrated that there was a significant modulation of its basal transcript levels in response to PAMP-mediated immune stimulation in hemocytes. Collectively, our findings indicate that AbAIF3 is a pro-apoptotic protein in abalones and is likely to be involved in host innate immune responses.

Acknowledgments

This research was supported by Golden Seed Project, Ministry of Agriculture, Food and Rural Affairs (MAFRA), Ministry of Oceans and Fisheries (MOF), Rural Development Administration (RDA) and Korea Forest Service (KFS).

References

[1] L.E. Broker, F.A. Kruyt, G. Giaccone, Cell death independent of caspases: a review. Clinical cancer research, official J. Am. Assoc. Cancer Res. 11 (2005) 3155–3162.
[2] P.H. Krammer, CD95's deadly mission in the immune system, Nature 407 (2000) 789–795.
[3] K. White, H. Steller, The control of apoptosis in Drosophila, Trends Cell Biol. 5 (1995) 74–78.
[4] E.W. Sun, Y.F. Shi, Apoptosis: the quiet death silences the immune system, Pharmacol. Ther. 92 (2001) 135–145.
[5] N.N. Danial, S.J. Korsmeyer, Cell death: critical control points, Cell. 116 (2004) 205–219.
[6] K. Terahara, K.G. Takahashi, Mechanisms and immunological roles of apoptosis in molluscs, Curr. Pharm. Des. 14 (2008) 131–137.
[7] M.J. McFall-Nagi, Consequences of evolving with bacterial symbionts: insights from the Squid-Vibrio associations, Annu. Rev. Ecol. Syst. 30 (1999) 235–256.
[8] M. Goedken, B. Morsey, I. Sunila, C. Dungan, S. De Guise, The effects of temperature and salinity on apoptosis of Crassostrea virginica hemocytes and Perkinsus marinus, J. Shellfish Res. 24 (2005) 177–183.
[9] I. Sunila, J. LaBanca, Apoptosis in the pathogenesis of infectious diseases of the eastern oyster Crassostrea virginica, Dis. Aquat. Organ 56 (2003) 163–170.
[10] M.D. Miramar, P. Costantini, L. Ravagnan, L.M. Saraiva, D. Haouzi, G. Brothers, et al., NADH oxidase activity of mitochondrial apoptosis-inducing factor, J. Biol. Chem. 276 (2001) 16391–16398.
[11] N. Vahsen, C. Cande, J.J. Briere, P. Benit, N. Joza, N. Larochette, et al., AIF deficiency compromises oxidative phosphorylation, EMBO J. 23 (2004) 4679–4689.
[12] N. Joza, G.Y. Oudit, D. Brown, P. Benit, Z. Kassiri, N. Vahsen, et al., Muscle-specific loss of apoptosis-inducing factor leads to mitochondrial dysfunction, skeletal muscle atrophy, and dilated cardiomyopathy, Mol. Cell. Biol. 25 (2005) 10261–10272.
[13] N. Joza, S.A. Susin, E. Daugas, W.L. Stanford, S.K. Cho, C.Y. Li, et al., Essential role of the mitochondrial apoptosis-inducing factor in programmed cell death,

Nature 410 (2001) 549–554.
[14] N. Modjtahedi, F. Giordanetto, F. Madeo, G. Kroemer, Apoptosis-inducing factor: vital and lethal, Trends Cell Biol. 16 (2006) 264–272.
[15] M. Wu, L.G. Xu, X. Li, Z. Zhai, H.B. Shu, AMID, an apoptosis-inducing factor-homologous mitochondrion-associated protein, induces caspase-independent apoptosis, J. Biol. Chem. 277 (2002) 25617–25623.
[16] Y. Ohiro, I. Garkavtsev, S. Kobayashi, K.R. Sreekumar, R. Nantz, B.T. Higashikubo, et al., A novel p53-inducible apoptogenic gene, PRG3, encodes a homologue of the apoptosis-inducing factor (AIF), FEBS Lett. 524 (2002) 163–171.
[17] Q. Xie, T. Lin, Y. Zhang, J. Zheng, J.A. Bonanno, Molecular cloning and characterization of a human AIF-like gene with ability to induce apoptosis, J. Biol. Chem. 280 (2005) 19673–19681.
[18] S.A. Susin, H.K. Lorenzo, N. Zamzami, I. Marzo, B.E. Snow, G.M. Brothers, et al., Molecular characterization of mitochondrial apoptosis-inducing factor, Nature 397 (1999) 441–446.
[19] H.K. Lorenzo, S.A. Susin, J. Penninger, G. Kroemer, Apoptosis inducing factor (AIF): a phylogenetically old, caspase-independent effector of cell death, Cell Death Differ. 6 (1999) 516–524.
[20] H.K. Lorenzo, S.A. Susin, Mitochondrial effectors in caspase-independent cell death, FEBS Lett. 557 (2004) 14–20.
[21] J.C. Dearlove, T.J. Betteridge, J.A. Henry, Stillbirth due to intravenous amphetamine, Bmj 304 (1992) 548.
[22] V.J. Yuste, R.S. Moubarak, C. Delettre, M. Bras, P. Sancho, N. Robert, et al., Cysteine protease inhibition prevents mitochondrial apoptosis-inducing factor (AIF) release, Cell death Differ. 12 (2005) 1445–1448.
[23] C. Delettre, V.J. Yuste, R.S. Moubarak, M. Bras, J.C. Lesbordes-Brion, S. Petres, et al., AIFsh, a novel apoptosis-inducing factor (AIF) pro-apoptotic isoform with potential pathological relevance in human cancer, J. Biol. Chem. 281 (2006) 6413–6427.
[24] N. Joza, J.A. Pospisilik, E. Hangen, T. Hanada, N. Modjtahedi, J.M. Penninger, et al., AIF: not just an apoptosis-inducing factor, Ann. N. Y. Acad. Sci. 1171 (2009) 2–11.
[25] A. Urbano, U. Lakshmanan, P.H. Choo, J.C. Kwan, P.Y. Ng, K. Guo, et al., AIF suppresses chemical stress-induced apoptosis and maintains the transformed state of tumor cells, EMBO J. 24 (2005) 2815–2826.
[26] M. Loeffler, E. Daugas, S.A. Susin, N. Zamzami, D. Metivier, A.L. Nieminen, et al., Dominant cell death induction by extramitochondrially targeted apoptosis-inducing factor, FASEB J. official Publ. Fed. Am. Soc. Exp. Biol. 15 (2001) 758–767.
[27] C. Delettre, V.J. Yuste, R.S. Moubarak, M. Bras, N. Robert, S.A. Susin, Identification and characterization of AIFsh2, a mitochondrial apoptosis-inducing factor (AIF) isoform with NADH oxidase activity, J. Biol. Chem. 281 (2006) 18507–18518.
[28] S. Wissing, P. Ludovico, E. Herker, S. Buttner, S.M. Engelhardt, T. Decker, et al., An AIF orthologue regulates apoptosis in yeast, J. Cell Biol. 166 (2004) 969–974.
[29] M. Byrne, M. Ho, E. Wong, N.A. Soars, P. Selvakumaraswamy, B. Shepard, et al., Unshelled abalone and corrupted urchins; development of marine calcifiers in a Changing Ocean, Proceedins R. Soc. Biol. Sci. Ser. B 278 (2011).
[30] R. van der Oost, J. Beyer, N.P. Vermeulen, Fish bioaccumulation and biomarkers in environmental risk assessment: a review, Environ. Toxicol. Pharmacol. 13 (2003) 57–149.
[31] P.C. Liu, Y.C. Chen, C.Y. Huang, K.K. Lee, Virulence of Vibrio parahaemolyticus isolated from cultured small abalone, Haliotis diversicolor supertexta, with withering syndrome, Lett. Appl. Microbiol. 31 (2000) 433–437.
[32] C.Y. Huang, P.C. Liu, K.K. Lee, Withering syndrome of the small abalone, Haliotis diversicolor supertexta, is caused by Vibrio parahaemolyticus and associated with thermal induction. Zeitschrift fur Naturforschung C, J. Biosci. 56 (2001) 898–901.
[33] T. Nakatsugawa, T. Nagai, K. Hiya, T. Nishizawa, K. Muroga, A virus isolated from juvenile Japanese black abalone Nordotis discus discus affected with amyotrophia, Dis. Aquat. Org. 36 (1999) 159–161.
[34] R.J.G. Goggin, L. Perkinsus, A protistan parasite of abalone in Australia, Mar. Freshw. Res. 46 (1995) 639–646.
[35] M. Droege, B. Hill, The Genome Sequencer FLX System–longer reads, more applications, straight forward bioinformatics and more complete data sets, J. Biotechnol. 136 (2008) 3–10.
[36] J.D. Thompson, D.G. Higgins, T.J. Gibson, CLUSTAL W: improving the sensitivity of progressive multiple sequence alignment through sequence weighting, position-specific gap penalties and weight matrix choice, Nucleic Acids Res. 22 (1994) 4673–4680.
[37] J.J. Campanella, L. Bitincka, J. Smalley, MatGAT: an application that generates similarity/identity matrices using protein or DNA sequences, BMC Bioinforma. 4 (2003) 29.
[38] K. Tamura, D. Peterson, N. Peterson, G. Stecher, M. Nei, S. Kumar, MEGA5: molecular evolutionary genetics analysis using maximum likelihood, evolutionary distance, and maximum parsimony methods, Mol. Biol. Evol. 28 (2011) 2731–2739.
[39] K.J. Livak, T.D. Schmittgen, Analysis of relative gene expression data using real-time quantitative PCR and the 2(-delta delta C(T)) method, Methods 25 (2001) 402–408.
[40] S.A. Bustin, V. Benes, J.A. Garson, J. Hellemans, J. Huggett, M. Kubista, et al., The MIQE guidelines: minimum information for publication of quantitative real-time PCR experiments, Clin. Chem. 55 (2009) 611–622.
[41] G. Koopman, C.P. Reutelingsperger, G.A. Kuijten, R.M. Keehnen, S.T. Pals, M.H. van Oers, Annexin V for flow cytometric detection of phosphatidylserine expression on B cells undergoing apoptosis, Blood 84 (1994) 1415–1420.
[42] L. Cunha, A. Amaral, V. Medeiros, G.M. Martins, F.F. Wallenstein, R.P. Couto, et al., Bioavailable metals and cellular effects in the digestive gland of marine limpets living close to shallow water hydrothermal vents, Chemosphere 71 (2008) 1356–1362.
[43] J.M. Hardwick, Apoptosis in viral pathogenesis, Cell Death Differ. 8 (2001) 109–110.
[44] S. Akira, S. Uematsu, O. Takeuchi, Pathogen recognition and innate immunity, Cell. 124 (2006) 783–801.
[45] S. Meyer, C. Temme, E. Wahle, Messenger RNA turnover in eukaryotes: pathways and enzymes, Crit. Rev. Biochem. Mol. Biol. 39 (2004) 197–216.
[46] R. Spooner, O. Yilmaz, The role of reactive-oxygen-species in microbial persistence and inflammation, Int. J. Mol. Sci. 12 (2011) 334–352.
[47] V. Nicaise, M. Roux, C. Zipfel, Recent advances in PAMP-triggered immunity against bacteria: pattern recognition receptors watch over and raise the alarm, Plant Physiol. 150 (2009) 1638–1647.
[48] J.A. Pospisilik, C. Knauf, N. Joza, P. Benit, M. Orthofer, P.D. Cani, et al., Targeted deletion of AIF decreases mitochondrial oxidative phosphorylation and protects from obesity and diabetes, Cell. 131 (2007) 476–491.
[49] D.D. Bannerman, S.E. Goldblum, Mechanisms of bacterial lipopolysaccharide-induced endothelial apoptosis, Am. J. physiology Lung Cell. Mol. Physiology 284 (2003) L899–L914.